

Mössbauer spectra of biotite from metapelites

M. DARBY DYAR

Department of Geological Sciences, University of Oregon, Eugene, Oregon 97403, U.S.A.

ABSTRACT

Mössbauer spectra of 52 biotite samples from metapelites of the Rangeley, Oquossoc, and Bryant Pond Quadrangles of northwestern Maine are examined to evaluate the oxidation state and site occupancies of Fe atoms. Spectra show nearly invariant peak positions for the *cis*-M2 site ($\delta = 1.13$ mm/s and $\Delta = 2.60$ mm/s) in the octahedral sheet of the biotite but greater variation in Fe²⁺ *trans*-M1 doublets ($\delta = 1.13$ mm/s and $\Delta = 1.95$ – 2.60 mm/s), which reflects a range of distortion in that site. Tetrahedral Fe³⁺ is present in amounts ranging from 4–14% of the total iron in all samples studied, roughly equivalent to the number of octahedral vacancies. Two octahedral Fe³⁺ doublets can be resolved in spectra for samples from the more oxidized assemblages studied. In more reduced rocks these doublets are poorly resolved and can be best represented by a single doublet with averaged hyperfine parameters. Fe³⁺/ΣFe remains constant within analytical errors among samples from lower garnet to potassium feldspar + sillimanite metamorphic grades as long as the oxide mineral phase does not change. However, octahedral Fe³⁺ content increases from a baseline of 4% of the total Fe in graphite-ilmenite-bearing assemblages up to 40% in biotites from hematite-bearing assemblages. The octahedral Fe²⁺ M2/M1 ratio that reflects ordering typically falls in a range from 2 to 3.5, but extremes of 1.14 up to 5.20 are observed in samples from sulfide-bearing or highly-oxidized assemblages.

INTRODUCTION

Historically the work of crystallographers and mineralogists has been oriented toward the analysis of individual samples considered to be representative of their localities. For this reason, too little is known about the correlation of crystallographic measurements (such as those gleaned from X-ray structure refinements or from Raman, FTIR, or Mössbauer spectroscopy) with petrologic data. Fortunately, there is some evidence to suggest links between petrogenetic context and crystal structure. For example, a recent review of Mössbauer studies of trioctahedral micas (Dyar, 1987) found that only 55 of 151 spectra reported in the literature noted some vague sample provenance (igneous or low grade were common descriptions); from these data a range of Fe site occupancies was noted, which appeared to be grossly related to sample locality and paragenesis. These observations prompted the author to undertake the present study to investigate the answers to the following questions:

1. How do oxidation state and site occupancies of Fe atoms in biotite vary on regional, local, and hand-sample scales? To what extent can a single specimen be considered representative of a region or a locality?

2. If Fe³⁺ content and cation ordering prove to demonstrate meaningful variability on any scale, can the variation be related to oxide assemblage, pressure, and temperature conditions in any systematic way?

To address these issues, Mössbauer spectra were obtained on 52 biotite samples from pelitic schists over a

range of assemblages (graphite-ilmenite, magnetite, and hematite-bearing) and metamorphic grades (lower garnet through potassium feldspar + sillimanite zone) mapped in northwestern Maine. This group of samples was specifically chosen because of existing detailed petrologic and major-element characterization by Guidotti and coworkers (Guidotti, 1984; Guidotti et al., 1977, 1988; Henry, 1981; Wood, 1981). This paper discusses the spectroscopic data for these samples. The petrologic implications are considered in Dyar et al. (1986, 1987) and in Guidotti and Dyar (in preparation).

EXPERIMENTAL DETAILS

The 52 biotite samples used in this study are from the Rangeley, Oquossoc, and Bryant Pond quadrangles of Northwestern Maine. They range through lower, middle, and upper garnet grades, lower and upper staurolite grades, a transition (staurolite + sillimanite) zone, lower and upper sillimanite grades, and potassium feldspar + sillimanite-grade metamorphic rocks (Guidotti et al., 1988). All rocks contain quartz and plagioclase and appear to have approached equilibrium. The majority of the samples (46) are from graphite-ilmenite-bearing assemblages (designated as Areas A and B; see Table 1), five samples contain magnetite (Area C), and one sample contains hematite (OB-16).

Major- and minor-element compositions of the biotite were determined by electron microprobe analysis at the University of Wisconsin–Madison, the University of Oregon, and the Smithsonian Astrophysical Observatory in

Cambridge, Massachusetts. Either Bence-Albee (1968) or Albee and Ray (1970) correction procedures were used. The acceleration potential was 15 keV, and sample currents ranged from 10 to 40 nA. Beam size was defocused to 10 μm to minimize alkali diffusion. Natural and synthetic minerals were used as standards for major elements, whereas synthetic glasses were used as standards for some minor elements. Duplicate analyses confirmed consistency among the instruments.

Biotite grains for Mössbauer analysis were separated from bulk crushed rocks using magnetic separation supplemented by hand-picking if needed. Approximately 200 mg of each pure separate were finely ground under acetone (to minimize possible oxidation of Fe) and mixed with sugar and acetone. Such a preparation coats individual grains with sugar to produce well-rounded particles, thereby alleviating preferred orientation in the plexiglass sample holder. For samples with finely intergrown coexisting phases such as ilmenite and garnet, it was often necessary to make successive Mössbauer measurements to ensure purity. Ultimately, pure separates were obtained from all the rocks studied.

Mössbauer spectra were recorded in 512 channels of two constant-acceleration Austin Science Associates spectrometers, one located in the Mineral Spectroscopy Laboratory at the Massachusetts Institute of Technology and one at the University of Oregon. Sources of 70–20 mCi ^{57}Co in Rh and Pd and gradients of approximately 0.01545 mm/s/channel were used. More than half the samples were run on both spectrometers, and there are no differences between spectra from the two instruments. At both locations results were calibrated against an α -Fe foil of 6 μm thickness and 99.99% purity. Spectra were fitted using different versions of the program STONE (Stone et al., 1984) on DEC LSI-11/73, MicroVax II, and IBM PS/2 MODEL 80 computers; no variation in the fits was obtained with the different computers. All three versions of the STONE program use a Gaussian, nonlinear regression procedure with the capability of constraining any set of parameters or linear combination of parameters. Lorentzian line shapes were used for resolving peaks, because there is no statistical justification for the addition of a Gaussian component to the curve shape used.

Procedures used to fit individual samples are described in detail in Dyar and Burns (1986). In brief, two-, three-, four-, and five-doublet fits (the last-named with doublets representing $\text{Fe}_{\text{M1}}^{2+}$, $\text{Fe}_{\text{M2}}^{2+}$, $\text{Fe}_{\text{M1}}^{3+}$, $\text{Fe}_{\text{M2}}^{3+}$, and $\text{Fe}_{\text{int}}^{2+}$) were attempted on each spectrum with gradually released constraints on widths and areas of peaks. Close attention was paid to the location and intensity of Fe^{3+} peaks. In some samples 30–50 different models were tested to ensure correct assignment of the smaller Fe^{3+} doublets. A statistical best fit was obtained for each sample using the χ^2 and MISFIT parameters (Ruby, 1973). The practical application of these statistical parameters is discussed elsewhere (Dyar, 1984). At best, the precision of the Mössbauer spectrometer and the fitting procedure is approximately ± 0.02 mm/s for isomer shift (δ) and quadrupole splitting

(Δ) and $\pm 1.5\%$ per peak for the area of well-resolved, distinct peaks (Dyar, 1984). However, the mica spectra presented here contain several substantially overlapping peaks. For this reason the errors are estimated to be as high as ± 0.05 mm/s and ± 0.03 mm/s for isomer shift and quadrupole splitting of Fe^{3+} and Fe^{2+} doublets, respectively. The errors for the areas of individual doublets are estimated to be ± 3 – 4% , based on replicate analyses and on comparisons of Mössbauer and wet chemical analyses of biotite samples from the Sierra Nevada batholith in central California (Dodge et al., 1969; Bancroft and Brown, 1975; Dyar and Burns, 1986).

RESULTS AND DISCUSSION

Mineral compositions reflecting both electron-microprobe and Mössbauer results are presented in Table 1. Mössbauer results for all samples are given in Table 2. In both tables, metamorphic zones and geographical areas (A, B, and C) are given following the designations of Guidotti et al. (1988).

Consistency of peak positions

The most striking characteristic of the Mössbauer results is the overall consistency of peak positions (Fig. 1), given the error estimates above and the standard deviations given in Table 2. In particular, the positions of the Fe^{2+} *cis*-M2 peaks are remarkably constant ($\delta = 1.13$ mm/s and $\Delta = 2.60$ mm/s), although the corresponding Fe^{2+} *trans*-M1 peaks vary over a wider range ($\delta = 1.13$ mm/s, $\Delta = 1.95$ – 2.60 mm/s). Standard deviations of parameters for the two doublets (0.02 mm/s for δ and 0.13 and 0.12 for Δ) are considerably smaller than the estimated errors of the measurements.

The nearly constant parameters of the *cis*-M2 doublets suggest that the Fe^{2+} site in different biotite samples is identical with respect to the s-electron density and electric-field gradient. Therefore, the electronic structure of the Fe atoms in the *cis*-M2 site (and the geometry of the O atoms surrounding them) is the same from sample to sample in this study (within the sensitivity of the Mössbauer technique). This confirms the conclusion drawn by Dyar (1987) from a literature survey. Apparently the environments around the iron atoms in the *cis*-M2 site are relatively invariant and independent of composition. In contrast, the greater variation in Mössbauer parameters of the M1 site indicates that Fe^{2+} in the M1 site resides in a more variable oxygen environment. Perhaps the *trans*-M1 site is more vulnerable to distortions caused by nearest neighbors owing to the *trans* configuration of its OH bonds.

Where the concentration of Fe^{3+} is sufficiently high, peak positions for those doublets are also quite consistent. For example, in the upper sillimanite grade samples from the Oquossoc quadrangle, Fe^{3+} doublets corresponding to the *cis*-M2 and *trans*-M1 sites are resolved, with parameters of $\delta \approx 0.42$ and 0.43 mm/s and $\Delta \approx 0.48$ and 1.09 mm/s, respectively. In some cases the two doublets cannot be distinctly resolved and can only be

TABLE 1. Biotite compositions recalculated with Fe³⁺

Sample name	RA-D75-66	RA-D72-66	RA-D9-66	RA-D28-66	RA-C95-66	RA-D86-66	RA-D11-66	RA-D37-66	RA-D12-66	RA-D14-66	RA-D60-66	RA-A65-66	RA-C1-66
Area	A	A	A	A	A	A	A	A	A	A	A	A	A
Zone	1	1	2	2	2	2	3	3	3	3	4	4	4
wt%													
SiO ₂	34.9	35.4	35.4	34.8	35.2	35.5	35.7	36.4	36.6	35.6	35.44	35.88	35.61
Al ₂ O ₃	19.7	19.4	19.6	19.9	19.7	19.6	19.9	19.8	19.9	20.1	19.61	19.45	19.72
FeO	19.7	19.9	19.3	20.0	21.2	19.8	17.5	16.4	17.8	19.1	17.77	18.24	17.21
Fe ₂ O ₃	3.57	3.31	2.93	3.62	2.05	3.00	4.55	3.73	3.76	3.17	3.21	2.25	3.38
MgO	8.00	6.77	7.70	7.46	8.02	7.38	8.24	9.61	7.96	9.65	8.75	9.30	9.58
TiO ₂	1.66	1.61	1.70	1.59	1.66	1.63	1.62	1.55	1.48	1.49	1.46	1.60	1.53
MnO	0.12	0.21	0.10	0.12	0.12	0.13	0.08	0.18	0.11	0.07	0.04	0.09	0.06
ZnO	0.00	0.11	0.09	0.00	0.00	0.07	0.09	0.09	0.00	0.11	0.07	0.07	0.00
K ₂ O	7.92	8.20	8.38	8.41	8.06	7.97	8.03	8.20	7.22	8.18	8.07	8.30	8.42
Na ₂ O	0.11	0.18	0.16	0.17	0.15	0.14	0.23	0.21	0.29	0.30	0.20	0.29	0.22
BaO	0.00	0.00	0.00	0.00	0.08	0.00	0.00	0.00	0.12	0.00	0.00	0.00	0.00
H ₂ O	3.95	3.92	3.94	3.95	3.95	3.93	3.99	4.04	3.99	4.05	3.94	3.98	4.30
Total	99.63	99.01	99.30	100.02	100.19	99.15	99.93	100.21	99.23	101.82	98.56	99.45	100.03
Number of atoms													
Si	5.30	5.42	5.39	5.29	5.33	5.41	5.36	5.41	5.50	5.28	5.39	5.41	5.36
Al (tet)	2.41	2.32	2.40	2.44	2.55	2.42	2.32	2.44	2.21	2.49	2.40	2.39	2.40
Fe ³⁺ (tet)	0.29	0.26	0.21	0.27	0.12	0.17	0.32	0.15	0.29	0.23	0.21	0.20	0.24
Total (tet)	8.00	8.00	8.00	8.00	8.00	8.00	8.00	8.00	8.00	8.00	8.00	8.00	8.00
Al (oct)	1.12	1.19	1.11	1.12	0.97	1.09	1.21	1.03	1.30	1.01	1.11	1.07	1.09
Fe ²⁺	2.51	2.55	2.46	2.55	2.69	2.53	2.20	2.04	2.23	2.36	2.26	2.30	2.16
Fe ³⁺ (oct)	0.12	0.12	0.12	0.15	0.12	0.17	0.19	0.27	0.13	0.05	0.16	0.05	0.13
Mg	1.81	1.55	1.75	1.69	1.81	1.68	1.85	2.13	1.78	2.13	1.98	2.09	2.14
Ti	0.19	0.19	0.19	0.18	0.19	0.19	0.18	0.17	0.17	0.17	0.17	0.18	0.17
Mn	0.02	0.03	0.01	0.02	0.02	0.02	0.01	0.02	0.01	0.01	0.01	0.01	0.01
Zn	0.00	0.01	0.01	0.00	0.00	0.01	0.01	0.01	0.00	0.01	0.01	0.01	0.00
Total (oct)	5.77	5.64	5.65	5.71	5.80	5.69	5.65	5.67	5.62	5.74	5.70	5.71	5.70
K	1.54	1.60	1.63	1.63	1.56	1.55	1.54	1.55	1.38	1.55	1.57	1.60	1.61
Na	0.03	0.05	0.05	0.05	0.04	0.04	0.07	0.06	0.08	0.09	0.06	0.09	0.06
Ba	0.00	0.00	0.00	0.00	0.01	0.00	0.00	0.00	0.01	0.00	0.00	0.00	0.00
Total (int)	1.57	1.65	1.68	1.68	1.61	1.59	1.61	1.61	1.47	1.64	1.63	1.69	1.67
Total	15.34	15.29	15.33	15.39	15.41	15.28	15.26	15.28	15.09	15.38	15.33	15.40	15.37

Sample name	RA-C4-66	RA-A73-66	RA-A14-66	RA-A69-66	RA-A33-66	RA-B53-66	RA-B48-66	RA-A57-66	RA-A96-66	RA-A93-66	RA-B4-66	RA-B41-66	RA-A95-66
Area	A	A	A	A	A	A	A	A	A	A	A	A	A
Zone	4	5	5	5	5	6	6	6	6	6	7	7	7
wt%													
Si	35.3	36.1	35.6	35.6	36.0	36.1	35.7	36.1	36.3	35.9	35.2	35.8	36.1
Al ₂ O ₃	20.2	20.0	20.1	20.2	20.0	19.7	19.5	20.0	20.0	20.2	20.1	20.2	20.4
FeO	18.6	17.1	17.6	18.1	16.8	16.2	17.7	16.3	18.8	17.8	19.3	18.8	19.1
Fe ₂ O ₃	2.82	2.34	2.41	1.99	2.08	2.46	1.48	2.70	1.82	3.50	1.37	1.10	1.35
MgO	9.03	10.1	9.65	9.2	10.2	10.4	9.85	10.1	8.59	8.73	9.64	9.23	9.45
TiO ₂	1.60	1.50	1.49	1.43	1.48	1.59	1.82	1.64	1.58	1.43	1.94	1.75	1.78
MnO	0.11	0.09	0.07	0.06	0.07	0.08	0.10	0.08	0.04	0.02	0.06	0.08	0.00
ZnO	0.00	0.13	0.11	0.10	0.11	0.12	0.11	0.10	0.00	0.00	0.00	0.12	0.00
K ₂ O	8.27	8.30	8.18	8.22	8.41	8.44	8.46	8.33	8.44	7.68	8.23	8.35	8.21
Na ₂ O	0.32	0.30	0.30	0.33	0.33	0.26	0.34	0.34	0.30	0.31	0.23	0.32	0.25
BaO	0.01	0.00	0.00	0.00	0.00	0.00	0.00	0.00	0.08	0.09	0.12	0.00	0.11
H ₂ O	3.99	4.03	3.99	3.97	4.00	4.00	3.97	4.02	3.99	4.00	3.99	3.99	4.04
Total	100.25	99.99	99.50	99.20	99.48	99.35	99.03	99.71	99.94	99.66	100.18	99.74	100.79
Number of atoms													
Si	5.30	5.37	5.35	5.37	5.39	5.40	5.39	5.39	5.44	5.38	5.28	5.38	5.37
Al (tet)	2.46	2.45	2.38	2.51	2.47	2.44	2.44	2.40	2.35	2.41	2.56	2.50	2.48
Fe ³⁺ (tet)	0.24	0.18	0.27	0.12	0.14	0.16	0.17	0.21	0.21	0.21	0.16	0.12	0.15
Total (tet)	8.00	8.00	8.00	8.00	8.00	8.00	8.00	8.00	8.00	8.00	8.00	8.00	8.00
Al (oct)	1.11	1.07	1.18	1.09	1.05	1.04	1.03	1.11	1.19	1.16	1.00	1.08	1.09
Fe ²⁺	2.34	2.12	2.21	2.28	2.11	2.03	2.24	2.03	2.36	2.23	2.43	2.36	2.37
Fe ³⁺ (oct)	0.08	0.10	0.00	0.10	0.09	0.12	0.00	0.09	0.00	0.18	0.00	0.00	0.00
Mg	2.02	2.24	2.16	2.07	2.28	2.32	2.22	2.24	1.92	1.95	2.16	2.07	2.09
Ti	0.18	0.17	0.17	0.16	0.17	0.18	0.21	0.18	0.18	0.16	0.22	0.20	0.20
Mn	0.01	0.01	0.01	0.01	0.01	0.01	0.01	0.01	0.01	0.00	0.01	0.01	0.00
Zn	0.00	0.01	0.01	0.01	0.01	0.01	0.01	0.01	0.00	0.00	0.00	0.01	0.00
Total (oct)	5.74	5.72	5.74	5.72	5.72	5.71	5.67	5.66	5.68	5.82	5.73	5.75	5.00
K	1.58	1.58	1.57	1.58	1.61	1.61	1.63	1.58	1.62	1.47	1.58	1.60	1.56
Na	0.09	0.09	0.09	0.10	0.10	0.08	0.10	0.10	0.09	0.09	0.07	0.09	0.07
Ba	0.00	0.00	0.00	0.00	0.00	0.00	0.00	0.00	0.01	0.01	0.01	0.00	0.01
Total (int)	1.67	1.67	1.66	1.68	1.71	1.69	1.73	1.68	1.72	1.57	1.66	1.69	1.64
Total	15.41	15.39	15.40	15.40	15.43	15.40	15.45	15.35	15.38	15.25	15.48	15.42	15.39

Note: Weight percentages of H₂O were calculated on the basis of 2(OH) and normalized to 22 O. Tetrahedral Fe³⁺ was determined from the area of the tetrahedral Fe³⁺ doublet (peak A0 on Table 2). Microprobe data represent averages of 10–20 analyses per biotite, depending on the instrument and the analyst. Standard deviations varied but are approximately 0.30 for SiO₂, 0.20 for Al₂O₃, 0.40 for FeO, 0.25 for MgO, 0.20 for TiO₂, 0.05 for

TABLE 1—Continued

Sample name	O-K-53	O-K-15	O-L-10	O-J-65	O-K-8'	O-K-8	O-K-9	O-C-30	O-C-26	O-C-14	O-C-18	O-K-10	9-8/7/63
Area	A	A	A	A	A	A	A	A	A	A	A	A	B
Zone	7'	7'	7'	7'	8*	8*	8*	8	8	8	8	8	8'
	wt%												
Si	35.8	35.6	35.2	35.2	37.3	37.1	37.9	35.3	35.5	35.2	35.4	35.1	36.6
Al ₂ O ₃	19.9	19.8	19.6	20.1	18.1	19.3	19.6	19.3	19.3	20.1	19.7	19.7	18.5
FeO	19.0	19.6	19.7	19.6	12.6	12.6	9.7	18.6	18.7	18.8	17.9	20.3	15.9
Fe ₂ O ₃	1.84	2.15	2.71	2.42	2.00	2.29	0.81	1.79	1.80	1.81	4.36	2.23	2.88
MgO	8.79	8.17	7.78	7.55	13.1	12.9	15.6	9.11	8.86	8.54	6.93	6.93	8.96
TiO ₂	1.72	1.80	1.73	2.03	2.18	2.20	1.97	2.34	2.46	2.33	2.62	2.62	1.85
MnO	0.19	0.21	0.05	0.06	0.32	0.32	0.48	0.17	0.20	0.13	0.13	0.12	0.08
ZnO	0.09	0.10	0.10	0.00	0.10	0.00	0.10	0.14	0.08	0.00	0.16	0.16	0.00
K ₂ O	8.46	8.23	8.27	8.60	9.63	9.62	9.30	8.94	8.84	8.81	8.47	8.71	8.37
Na ₂ O	0.29	0.27	0.27	0.22	0.09	0.07	0.17	0.23	0.28	0.25	0.25	0.22	0.25
BaO	0.00	0.00	0.00	0.07	0.00	0.08	0.00	0.00	0.00	0.02	0.00	0.00	0.00
H ₂ O	3.99	3.97	3.94	3.95	4.06	4.10	4.15	3.97	3.97	3.97	3.97	3.94	3.93
Total	100.07	99.90	99.35	99.80	99.48	100.58	99.78	99.89	99.99	99.96	99.89	100.03	97.32
	Number of atoms												
Si	5.38	5.38	5.36	5.33	5.51	5.42	5.48	5.34	5.36	5.30	5.37	5.33	5.59
Al (tet)	2.52	2.54	2.47	2.53	2.35	2.38	2.43	2.51	2.44	2.54	2.64	2.47	2.13
Fe ³⁺ (tet)	0.10	0.08	0.17	0.14	0.14	0.20	0.09	0.15	0.20	0.16	0.19	0.20	0.28
Total (tet)	8.00	8.00	8.00	8.00	8.00	8.00	8.00	8.00	8.00	8.00	8.00	8.00	8.00
Al (oct)	1.01	0.98	1.05	1.06	0.80	0.94	0.90	0.93	0.99	1.03	1.05	1.06	1.19
Fe ²⁺	2.39	2.48	2.51	2.49	1.56	1.55	1.17	2.35	2.36	2.37	2.26	2.58	2.03
Fe ³⁺	0.10	0.16	0.14	0.14	0.09	0.05	0.00	0.05	0.00	0.05	0.30	0.06	0.05
Mg	1.97	1.84	1.76	1.71	2.90	2.81	3.35	2.05	1.99	1.92	1.56	1.57	2.04
Ti	0.19	0.20	0.20	0.23	0.24	0.24	0.21	0.27	0.28	0.26	0.30	0.30	0.21
Mn	0.02	0.03	0.01	0.01	0.04	0.04	0.06	0.02	0.03	0.02	0.02	0.02	0.01
Zn	0.01	0.01	0.01	0.00	0.01	0.00	0.01	0.02	0.01	0.00	0.02	0.02	0.00
Total (oct)	5.69	5.70	5.68	5.64	5.64	5.63	6.70	5.69	5.66	5.65	5.51	5.61	5.53
K	1.62	1.59	1.61	1.66	1.82	1.80	1.72	1.72	1.70	1.70	1.63	1.69	1.63
Na	0.09	0.08	0.08	0.07	0.03	0.02	0.05	0.07	0.08	0.07	0.07	0.07	0.07
Ba	0.00	0.00	0.00	0.00	0.00	0.01	0.00	0.00	0.00	0.00	0.00	0.00	0.00
Total (int)	1.71	1.67	1.69	1.73	1.85	1.83	1.77	1.79	1.78	1.77	1.70	1.76	1.70
Total	15.40	15.37	15.37	15.37	15.49	15.46	15.47	15.48	15.44	15.42	15.21	15.37	15.23

Sample name	16- 8/23/60	4- 7/26/59	16- 7/18/60	15- 8/18/59	14- 7/2/60	5- 9/20/61	O-b-41	O11	OG92	OH49P	OH56	OH72	OB16
Area	B	B	B	B	B	B	B	C	C	C	C	C	C
Zone	8'	8'	9	9	9	9	-	-	-	-	-	-	-
	wt%												
SiO ₂	36.3	34.5	34.4	35.9	35.3	34.6	36.8	35.4	35.3	35.5	35.0	35.2	36.7
Al ₂ O ₃	18.7	18.6	19.9	19.5	19.1	19.0	17.5	19.7	19.9	19.3	19.2	18.6	19.2
FeO	16.7	17.6	17.2	15.1	18.0	17.0	20.6	15.0	14.9	14.8	14.1	15.5	7.45
Fe ₂ O ₃	3.54	3.18	2.36	1.46	2.73	3.33	3.42	4.17	3.89	4.90	5.79	5.13	7.05
MgO	7.95	8.16	8.40	10.6	6.49	6.61	6.15	9.61	9.97	9.93	9.72	9.17	12.9
TiO ₂	2.06	2.44	2.94	3.24	3.58	3.07	2.26	1.57	1.45	1.78	2.03	2.31	1.32
MnO	0.20	0.29	0.16	0.32	0.19	0.21	1.03	0.22	0.19	0.24	0.21	0.30	0.23
ZnO	0.00	0.00	0.00	0.06	0.00	0.00	0.00	0.07	0.07	0.08	0.06	0.03	0.10
K ₂ O	8.45	9.08	9.44	9.38	9.15	8.70	9.46	8.90	9.00	8.97	8.96	9.29	7.34
Na ₂ O	0.36	0.27	0.16	0.10	0.12	0.21	0.02	0.20	0.21	0.25	0.18	0.14	0.18
BaO	0.00	0.00	0.00	0.14	0.00	0.00	0.06	0.10	0.11	0.12	0.22	0.17	0.05
H ₂ O	3.94	3.88	3.93	4.02	3.92	3.85	3.96	3.97	3.98	4.00	3.98	3.97	4.03
Total	98.20	98.00	98.89	99.82	98.58	96.58	101.26	98.91	98.97	99.87	99.45	99.81	96.55
	Number of atoms												
Si	5.52	5.34	5.25	5.34	5.41	5.40	5.58	5.35	5.33	5.32	5.27	5.33	5.47
Al (tet)	2.12	2.48	2.48	2.60	2.41	2.27	2.13	2.46	2.51	2.46	2.49	2.37	2.43
Fe ³⁺ (tet)	0.36	0.18	0.27	0.06	0.18	0.33	0.29	0.19	0.16	0.22	0.24	0.30	0.10
Total (tet)	8.00	8.00	8.00	8.00	8.00	8.00	8.00	8.00	8.00	8.00	8.00	8.00	8.00
Al (oct)	1.24	0.91	1.09	0.83	1.04	1.22	0.99	1.04	1.02	0.95	0.93	0.94	0.93
Fe ²⁺	2.13	2.28	2.19	1.89	2.30	2.21	2.61	1.90	1.88	1.85	1.78	1.95	0.93
Fe ³⁺ (oct)	0.05	0.19	0.00	0.10	0.13	0.05	0.10	0.28	0.28	0.34	0.41	0.28	0.69
Mg	1.81	1.88	1.91	2.36	1.48	1.54	1.39	2.16	2.24	2.22	2.18	2.07	2.86
Ti	0.24	0.28	0.34	0.36	0.41	0.36	0.26	0.18	0.16	0.20	0.23	0.26	0.15
Mn	0.03	0.04	0.02	0.04	0.03	0.03	0.13	0.03	0.02	0.03	0.03	0.04	0.03
Zn	0.00	0.00	0.00	0.01	0.00	0.00	0.00	0.01	0.01	0.01	0.01	0.01	0.01
Total (oct)	5.50	5.58	5.55	5.59	5.39	5.41	5.48	5.60	5.61	5.60	5.57	5.55	5.60
K	1.64	1.79	1.84	1.78	1.79	1.73	1.83	1.72	1.73	1.72	1.72	1.79	1.39
Na	0.11	0.08	0.05	0.03	0.04	0.06	0.01	0.06	0.06	0.07	0.05	0.04	0.05
Ba	0.00	0.00	0.00	0.01	0.00	0.00	0.00	0.01	0.01	0.01	0.01	0.01	0.00
Total (int)	1.75	1.87	1.89	1.82	1.83	1.79	1.84	1.79	1.80	1.80	1.78	1.84	1.44
Total	15.25	15.45	15.44	15.41	15.22	15.20	15.32	15.39	15.41	15.40	15.35	15.39	15.04

MnO, 0.05 for ZnO, 0.15 for K₂O, 0.06 for Na₂O, and 0.05 for BaO. Significant digits are tabulated using the general convention of two significant digits after the decimal point for wt% oxides <10.0 and one digit for ≥10.0. Relative atom numbers are presented with two places after the decimal for consistency; it is impossible to accurately estimate their accuracy given the uncertainties in H and O content of these samples.

TABLE 2. Mössbauer data

Sample	Zone	IS 0	QS 0	A 0	IS 1	QS 1	A 1	IS 2	QS 2	A 2	IS 3	QS 3	A 3
Ra-d75-66	1	0.14	0.17	10	—	—	—	0.40	0.93	4	1.07	2.29	23
Ra-d72-66	1	0.14	0.18	9	—	—	—	0.39	0.94	4	1.07	2.23	19
Ra-d9-66	2	0.15	0.20	7	—	—	—	0.38	0.78	5	1.08	2.30	22
Ra-d28-66	2	0.07	0.31	9	0.41	0.71	5	—	—	—	1.09	2.19	21
Ra-c95-66	2	0.14	0.26	4	0.37	0.68	2	0.45	0.94	2	1.14	2.26	31
Ra-d86-66	2	0.21	0.20	6	—	—	—	0.43	0.84	6	1.09	2.36	24
Ra-d11-66	3	0.14	0.21	12	—	—	—	0.39	0.95	7	1.07	2.32	30
Ra-d37-66	3	0.18	0.68	6	0.37	0.68	7	0.39	1.23	4	1.09	2.24	21
Ra-d12-66	3	0.09	0.20	11	—	—	—	0.38	0.83	5	1.06	2.30	20
Ra-d14-66	3	0.11	0.25	11	—	—	—	0.40	0.84	2	1.08	2.27	22
Ra-d60-66	4	0.15	0.21	8	—	—	—	0.38	0.84	6	1.07	2.26	17
Ra-a65-66	4	0.13	0.18	8	0.39	0.69	2	—	—	—	1.09	2.25	20
Ra-c1-66	4	0.14	0.19	10	—	—	—	0.39	0.87	5	1.02	2.23	21
Ra-c4-66	4	0.09	0.23	9	0.44	0.71	3	—	—	—	1.08	2.26	24
Ra-a73-66	5	0.19	0.16	7	0.40	0.91	4	—	—	—	1.09	2.21	22
Ra-a14-66	5	0.08	0.21	11	—	—	—	—	—	—	1.08	2.23	20
Ra-a69-66	5	0.23	0.19	5	—	—	—	0.35	0.99	4	1.10	2.19	21
Ra-a33-66	5	0.21	0.18	6	—	—	—	0.37	1.10	4	1.09	2.17	20
Ra-b53-66	6	0.15	0.35	7	—	—	—	0.38	0.92	5	1.12	2.17	20
Ra-b48-66	6	0.15	0.16	7	—	—	—	—	—	—	1.09	2.22	22
Ra-a57-66	6	0.13	0.22	9	—	—	—	0.39	0.90	4	1.06	2.33	29
Ra-a96-66	6	0.13	0.22	8	—	—	—	—	—	—	1.10	2.30	24
Ra-a93-66	6	0.16	0.21	8	0.39	0.80	4	0.38	1.29	3	1.05	2.26	19
Ra-B4-66	7	0.05	0.29	6	—	—	—	—	—	—	1.12	2.29	43
Ra-B41-66	7	0.19	0.27	5	—	—	—	—	—	—	1.10	2.22	32
Ra-A95-66	7	0.05	0.28	6	—	—	—	—	—	—	1.11	2.30	44
O-K-53	7'	0.20	0.45	4	—	—	—	0.43	0.97	4	1.10	2.04	17
O-K-15	7'	0.20	0.49	3	—	—	—	0.43	1.06	6	1.10	2.11	28
O-L-10	7'	0.21	0.16	6	—	—	—	0.40	0.87	5	1.09	2.22	25
O-J-65	7'	0.16	0.25	5	0.43	0.60	5	—	—	—	1.06	2.20	24
O-K-8'	8*	0.19	0.23	8	—	—	—	0.38	0.82	5	1.09	2.29	33
O-K-8	8*	0.07	0.19	11	—	—	—	0.39	1.01	3	1.09	2.31	33
O-K-9	8*	0.09	0.32	7	—	—	—	—	—	—	1.11	2.13	15
O-C-30	8	0.11	0.35	6	—	—	—	0.38	1.21	2	1.11	2.13	22
O-C-26	8	0.17	0.56	8	—	—	—	—	—	—	1.09	2.08	25
O-C-14	8	0.16	0.13	6	—	—	—	0.41	0.93	2	1.09	2.21	23
O-C-18	8	0.15	0.34	7	—	—	—	0.35	0.85	11	1.13	2.09	17
O-K-10	8	0.19	0.14	7	—	—	—	0.34	0.86	2	1.09	2.20	28
9-8/7/63	8'	0.13	0.16	12	—	—	—	0.39	0.92	2	1.06	2.21	23
16-8/23/60	8'	0.12	0.18	14	—	—	—	0.47	1.01	2	1.06	2.25	24
4-7/26/59	8'	0.20	0.14	7	—	—	—	0.37	0.90	7	1.11	2.21	24
16-7/18/60	9	0.13	0.16	11	—	—	—	—	—	—	1.07	2.21	25
15-8/18/59	9	0.16	0.28	5	0.43	0.57	8	—	—	—	1.09	2.22	25
14-7/2/60	9	0.15	0.34	7	—	—	—	0.38	0.78	5	1.10	2.09	21
5-9/20/61	9	0.14	0.18	13	0.38	0.49	2	—	—	—	1.06	2.22	25
O-b-41	—	0.13	0.33	11	0.38	0.73	2	0.39	1.34	2	1.08	2.34	27
O11	—	0.13	0.22	8	0.38	0.63	7	0.39	1.19	5	1.13	2.59	64
OG92	—	0.15	0.15	7	0.36	0.78	7	0.38	1.23	5	1.12	2.58	65
OH49'	—	0.13	0.19	9	0.38	0.63	8	0.39	1.03	6	1.12	2.60	58
OH56	—	0.13	0.24	10	0.38	0.58	7	0.39	1.06	10	1.12	2.58	56
OH72	—	0.16	0.19	12	0.39	0.74	7	0.38	1.21	4	1.13	2.58	56
OB16	—	0.16	0.64	6	0.38	0.76	28	0.41	1.27	12	1.12	1.95	9
Ave. Rangeley	—	0.15	0.25	7.8	0.40	0.68	4.2	0.39	0.94	4.3	1.09	2.22	24.2
SD Rangeley	—	0.04	0.11	2.5	0.02	0.11	2.0	0.03	0.13	2.0	0.02	0.07	5.9
Ave. all samples	—	0.15	0.25	8.0	0.39	0.69	6.4	0.39	0.99	4.7	1.09	2.26	27.4
SD all samples	—	0.04	0.12	2.5	0.02	0.10	5.8	0.03	0.16	2.4	0.02	0.13	12.2

Note: Zone = Metamorphic grade: 1 = lower garnet, 2 = middle garnet, 3 = upper garnet, 4 = lower staurolite, 5 = upper staurolite, 6 = transition zone, 7 = lower sillimanite (1–7 from Rangeley quadrangle), 7' = lower sillimanite, 8* = sulfide-bearing lower sillimanite, 8 = upper sillimanite (7'–8 from Oquossoc quadrangle), 8' = upper sillimanite, 9 = potassium feldspar + sillimanite (8' and 9 from Bryant Pond quadrangle). IS = isomer shift, QS = quadrupole splitting, A = peak area (in % of total area). Peaks 0–4 represent Fe²⁺ in tetrahedral, octahedral M2, and octahedral M1 sites and Fe²⁺ in octahedral M1 and octahedral M2 sites. % MIS = % MISFIT, and % UN = % uncertainty in the fit (see Ruby, 1973).

fitted as one merged doublet with averaged parameters of $\delta \approx 0.42$ mm/s and $\Delta \approx 0.85$ mm/s.

M2/M1 ratios

Because the higher velocity Fe²⁺ peaks are not overlapped by Fe³⁺ peaks, it is possible to determine relative site occupancies with some confidence (± 0.4 – 0.6). The ratio of Fe²⁺ in M2 to that in M1 (M2/M1) ranges from

a low of 1.14 to a high of 5.20, with an average value of 2.91. In these samples, there are few biotites with the 2:1 ratio that would be predicted by equipoint ranks for IM biotite. There are 45 biotite samples in our data set that have greater than twice the amount of Fe²⁺ in M2 than in M1, but there are also seven samples for which the reverse is true. Previously published ranges of Fe²⁺ M2/M1 site occupancy ratios are similar to those of the Maine

TABLE 2—Continued

IS 4	QS 4	A 4	% MIS	% UN	M2/M1	% Fe ³⁺
1.12	2.62	62	0.09	0.01	2.70	14.0
1.12	2.60	68	0.02	0.01	3.58	13.0
1.13	2.62	65	0.03	0.01	2.95	12.0
1.13	2.60	67	0.11	0.02	3.19	14.0
1.14	2.61	60	0.08	0.01	1.94	8.0
1.14	2.69	64	0.10	0.03	2.66	12.0
1.13	2.63	50	0.15	0.02	1.68	19.0
1.13	2.61	62	-0.15	-0.02	2.95	17.0
1.12	2.61	63	0.28	0.01	3.13	16.0
1.13	2.62	64	0.13	0.02	2.90	13.0
1.12	2.61	69	0.02	0.01	4.06	14.0
1.13	2.61	70	0.09	0.01	3.50	10.0
1.12	2.59	64	0.00	0.00	3.05	15.0
1.12	2.61	64	0.16	0.02	2.66	12.0
1.12	2.59	67	0.09	0.01	3.05	11.0
1.12	2.60	69	0.11	0.02	3.45	11.0
1.13	2.61	70	-0.06	-0.02	3.33	9.0
1.13	2.61	70	-0.52	-0.07	3.50	10.0
1.13	2.60	68	0.27	0.01	3.40	12.0
1.13	2.59	70	-0.06	-0.01	3.18	7.0
1.13	2.64	58	0.25	0.01	2.00	13.0
1.13	2.66	68	-1.08	-0.15	2.83	8.0
1.12	2.60	66	0.18	0.01	3.47	15.0
1.13	2.63	51	-0.06	-0.02	1.19	6.0
1.13	2.60	63	-0.02	-0.01	1.97	5.0
1.13	2.62	50	-0.41	-0.07	1.14	6.0
1.11	2.56	75	0.20	0.03	4.41	8.0
1.10	2.57	63	0.09	0.02	2.25	9.0
1.12	2.60	64	0.15	0.01	2.50	11.0
1.10	2.57	66	0.09	0.02	2.75	10.0
1.13	2.63	53	0.01	0.01	1.60	13.0
1.12	2.64	53	-0.03	-0.01	1.61	14.0
1.12	2.58	78	0.11	0.03	5.20	7.0
1.13	2.57	70	0.10	0.01	3.18	8.0
1.11	2.55	66	0.16	0.03	2.64	8.0
1.12	2.59	68	-0.22	-0.03	2.96	8.0
1.12	2.57	63	-0.05	-0.02	3.70	18.0
1.12	2.59	63	-0.05	-0.01	2.25	9.0
1.12	2.58	62	0.06	0.01	2.70	14.0
1.12	2.59	60	0.01	0.01	2.50	16.0
1.14	2.65	62	-0.01	-0.03	2.58	14.0
1.12	2.58	64	0.02	0.01	2.56	11.0
1.13	2.62	61	0.04	0.01	2.44	11.0
1.12	2.57	67	-0.06	-0.02	3.19	12.0
1.12	2.58	68	0.04	0.01	2.72	15.0
1.14	2.64	57	0.04	0.01	2.11	15.0
1.06	2.24	16	0.04	0.01	4.00	20.0
1.08	2.17	17	0.11	0.01	3.82	19.0
1.06	2.24	18	0.16	0.01	3.22	23.0
1.06	2.20	17	0.06	0.01	3.29	27.0
1.04	2.26	21	0.05	0.01	2.67	23.0
1.13	2.54	45	0.27	0.02	5.00	46.0
1.12	2.60	64.2	na	na	2.83	11.4
0.01	0.03	5.9	na	na	0.78	3.4
1.12	2.57	59.2	na	na	2.91	13.2
0.02	0.12	14.9	na	na	0.82	6.5

biotite samples (Dyar, 1987 for trioctahedral micas; DeGrave et al., 1987 for chlorites). Thus, the data support the observation that Fe²⁺ is more commonly found in M2 than in M1 sites. This does not necessarily imply that Fe²⁺ has a *cis*-M2 site preference. It is equally likely that some other cation (or cations) has a site preference and that Fe²⁺ is randomly occupying the remaining available sites. Additional support for this idea is the observation (Tables 1 and 2) that ordering of Fe²⁺ in M1 and M2 does not appear to vary with metamorphic grade, Ti content, or Fe²⁺/Mg ratio. The observed ordering is caused by some more complicated (or less obvious) cause. Un-

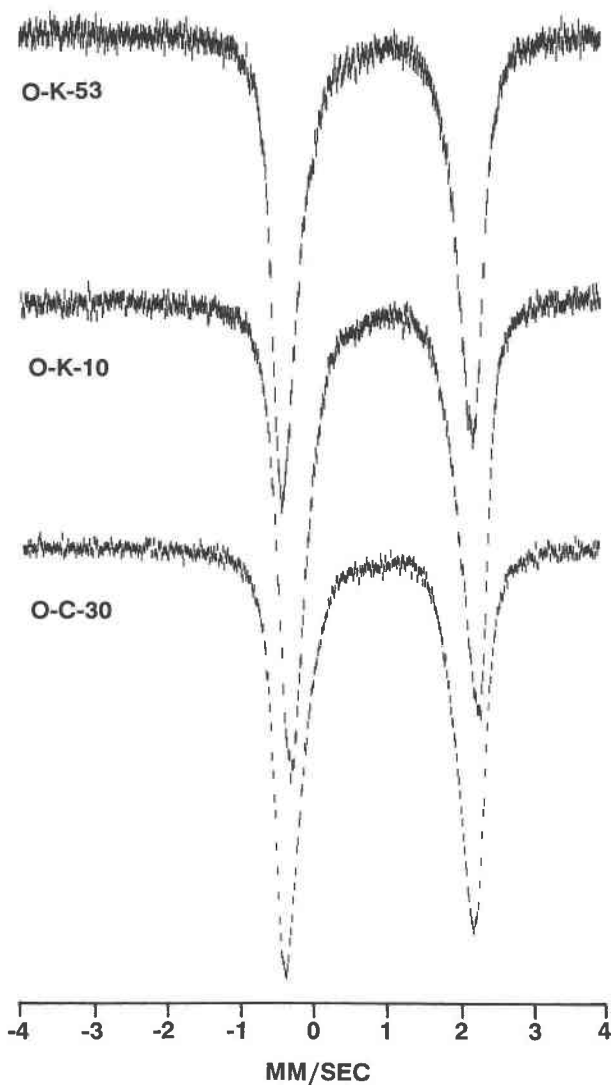


Fig. 1. Three nearly identical Mössbauer spectra of biotite samples from the upper sillimanite zone of the Oquossoc quadrangle. Fits of these data are identical well within the known precision of the Mössbauer technique.

fortunately the compositions of these biotite samples are too complex to allow assignment of site preferences to individual cations.

Owing to the small areas and extensive overlap of the peaks for Fe³⁺, quantitative conclusions about the distribution of Fe³⁺ between the *cis*-M2 and *trans*-M1 sites in the octahedral sheet cannot be drawn.

Tetrahedral Fe³⁺

The presence of tetrahedral Fe³⁺ in amounts ranging from 0.09 to 0.37 cations per formula unit (based on 22 O) was confirmed in all 52 of the samples studied (Fig. 2B). This result is unexpected given that all of our samples are saturated with respect to Al and therefore contain sufficient Al³⁺ to fill the tetrahedral site. Because the Al³⁺

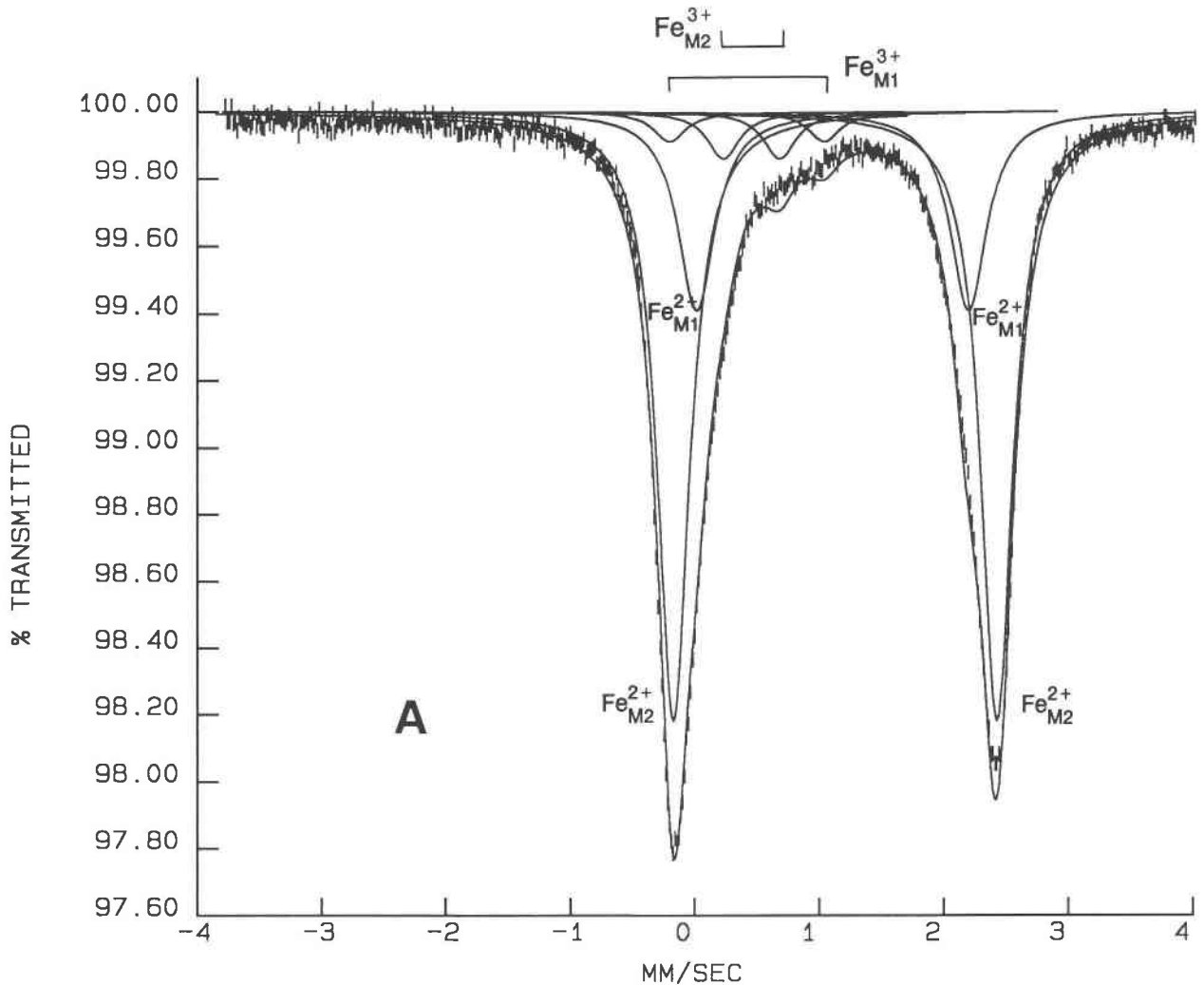


Fig. 2. Two fits to the same Mössbauer spectrum of biotite O-L-10. The fit shown above (A) has two doublets representing Fe^{2+} and two doublets representing Fe^{3+} , all in the octahedral sheet. The fit at the right (B) has only one octahedral Fe^{3+} doublet and one tetrahedral Fe^{3+} doublet. Even by visual inspection it is clear that the latter fit is superior; this conclusion is borne out by the statistics of the fit.

cation (0.39 \AA) is so much smaller than Fe^{3+} (0.49 \AA) in tetrahedral coordination (Shannon, 1976), it seems improbable that Fe^{3+} would preferentially substitute for Al^{3+} . However, the Mössbauer data presented here and in numerous examples in the literature (e.g., Ferrow, 1987) can consistently be fitted with tetrahedral peaks. Either there is a problem with the interpretation of the Mössbauer data, or some unconsidered factor is favoring Fe^{3+} occupancy of the tetrahedral sites.

Previous work by Dyar and Burns (1986) has sought to clarify the interpretation of Mössbauer data for biotite through study of synthetic and naturally occurring end-member annites and ferriannites in which Al-deficient stoichiometries necessitate tetrahedral Fe^{3+} . This past work, coupled with a literature review of Mössbauer data

for trioctahedral micas (Dyar, 1987) has established firmly the expected position of tetrahedral Fe^{3+} peaks in phyllosilicate spectra. These peak positions are similar to those of four-coordinated Fe^{3+} in other silicates such as feldspars (Levitz et al., 1980; Huggins, 1976) and sillimanite (Rossman et al., 1982). Therefore, it seems unlikely that our interpretation of the Mössbauer data is incorrect.

It seems equally unlikely that our well-developed understanding of mica crystal chemistry is incorrect. Average octahedral cation radii in these samples range from 0.70 to 0.72 \AA (roughly the ionic radius of Mg^{2+}), if vacancies are considered to have ionic radii of about 0.80 \AA (Guggenheim, 1984). This size range is roughly in the middle of the range of that of all observed natural mica compositions and is similar to that of pure phlogopite.

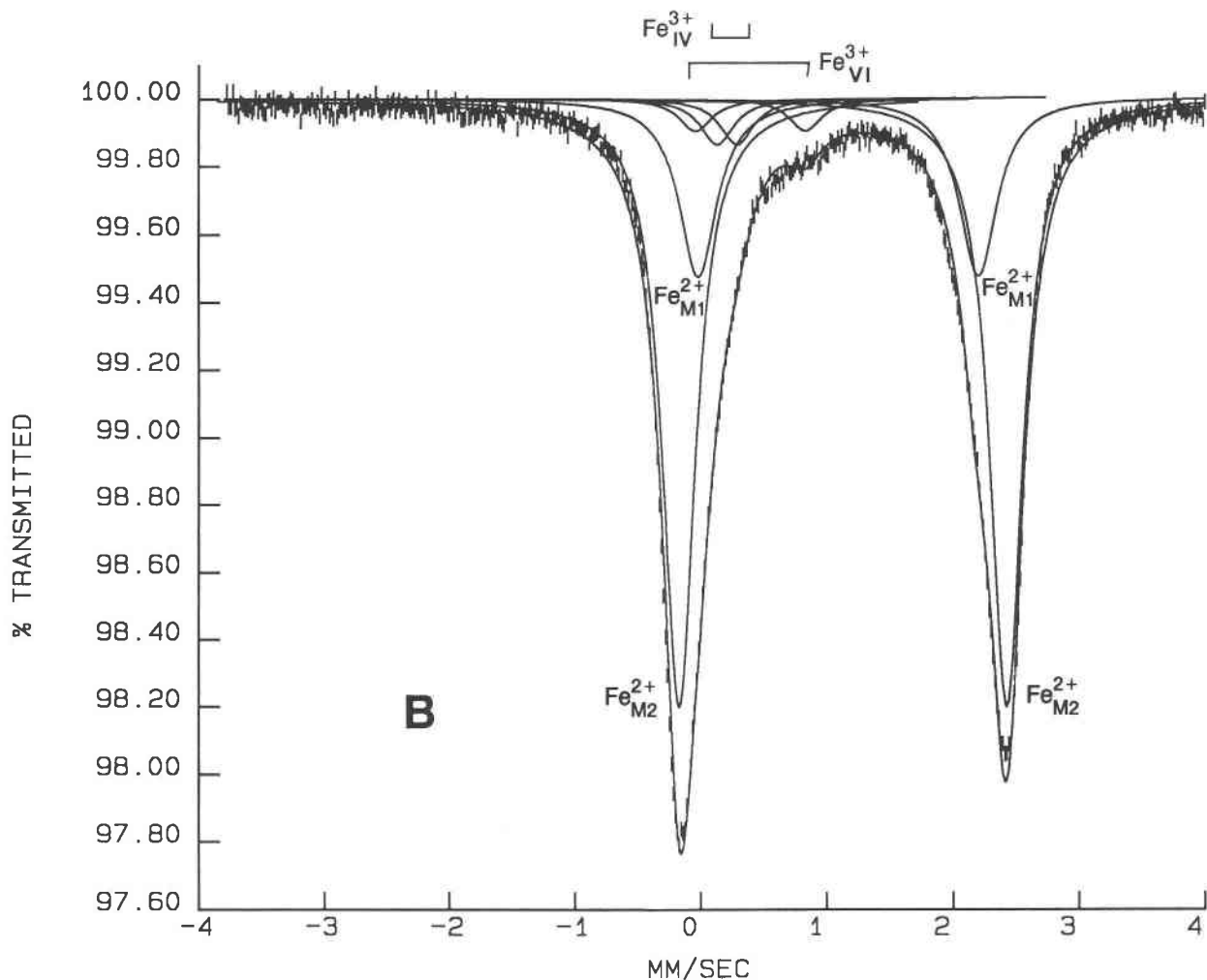


Fig. 2.—Continued.

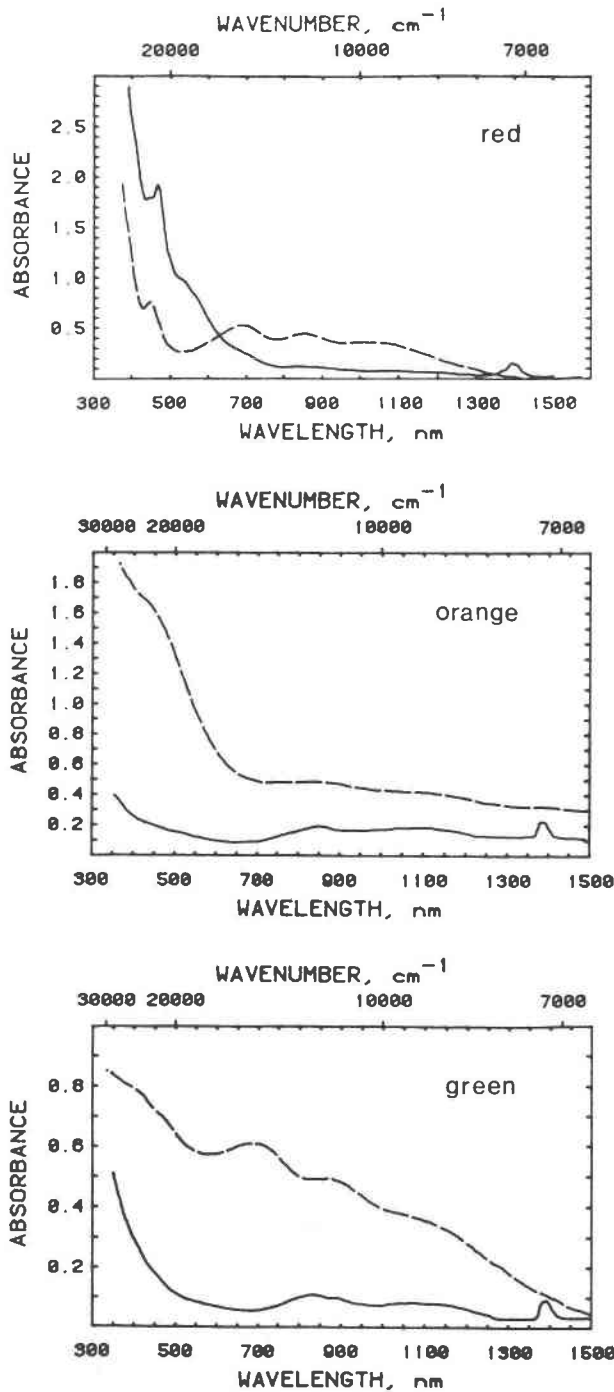
In this octahedral cation size range the lateral dimension of the octahedral sheet is larger than that of the $AlSi_3$ tetrahedral sheet, and rotation of adjacent tetrahedra within the plane of the sheet must occur in order to reduce the lateral dimensions of the tetrahedral sheet. Therefore, if the average octahedral ionic radius of 0.71 Å is used to predict site occupancies in these samples, tetrahedral Fe^{3+} would certainly not be expected because its presence would only enlarge the size of the tetrahedra and increase the size mismatch between the tetrahedral and octahedral sheets. Thus, arguments based on average octahedral ionic radii cannot explain the presence of tetrahedral Fe^{3+} .

However, because of the complex compositions of these micas, local structural environments may be very different from the average structure. Some local compositions may optimize the fit between tetrahedral and octahedral sheets. The number of tetrahedral Fe^{3+} cations per formula unit is relatively small (0.1–0.3 Fe^{3+} per eight tet-

rahedral cations). Therefore a distortion of only one in 27–80 sites would be required to accommodate the observed tetrahedral Fe^{3+} contents.

A likely candidate for the cause of such a local distortion is a vacancy in the octahedral sheet. In $2M_1$ muscovite, for instance, there are two Al atoms and one vacancy corresponding to the three octahedral sites (two M_2 and one M_1 , respectively). Shared edges between occupied octahedra are shortened (Bailey, 1984). Thus, the entire sheet is thinned in the *c* direction and expanded in the *a-b* plane.

In contrast, octahedral vacancies in trioctahedral micas are less commonly observed (0.2–0.4 vacancies per six octahedral cations), so overall structural adjustments of the type found in muscovite would not be expected. However, local scale adjustments probably occur because vacant octahedra are large and edge lengths of the coordination polyhedra will therefore be longer. Local scale adjustments of the tetrahedra in the vicinity of the en-



larged octahedra will also be required. Perhaps local adjustment of the geometry of the tetrahedral sites creates a larger or more distorted fourfold site that can as easily accommodate Fe^{3+} as Al^{3+} . The striking similarity between the concentration of tetrahedral Fe^{3+} and that of octahedral vacancies strongly suggests that the two are related.

Additional corroboration for the assignment of Fe^{3+} to tetrahedral coordination comes from the color of the mi-

←

Fig. 3. Visible-region absorption spectra of mica thin sections (cut normal to the cleavage) showing absorption owing to O, Fe^{3+} , Fe^{2+} , and Ti^{4+} . The top spectrum of an Al-deficient Fe^{3+} -bearing clintonite shows absorption bands at 22700, 20300, and 19200 cm^{-1} (characteristic of tetrahedral Fe^{3+}) superimposed on the tail of a UV band, which is most likely owing to Fe^{3+} -O charge transfer (Rossman, 1984). The middle spectrum has strong absorption in the 20000–24000 cm^{-1} region, which is characteristic of Ti^{4+} - Fe^{2+} interactions. The bottom spectrum has peaks at 9000, 11000, and 14000 cm^{-1} , which represent contributions from Fe^{2+} and Fe^{3+} - Fe^{2+} charge transfer. Sample thicknesses are 374, 181, and 209 μm , respectively. Solid lines represent light polarized parallel to cleavage, dashed lines represent light perpendicular to cleavage.

cas. Biotite from our graphite- and ilmenite-bearing rocks tends to be red-orange in plane-polarized light, whereas the biotite that coexists with magnetite and hematite (corresponding to more highly oxidizing conditions) is green. For the most part these colors arise from interactions among O, Fe^{3+} , Fe^{2+} , and Ti^{4+} ions. Typical optical absorption spectra of micas are shown in Figure 3. Biotite with a large Ti^{4+} concentration absorbs strongly in the 20000–24000 cm^{-1} region of the visible region spectrum, transmitting the red-orange color commonly associated with Ti (Guidotti, 1984). This color is the result of interaction between Fe^{2+} and Ti^{4+} (Faye, 1968) accompanied by substitutional broadening of the Fe-O charge-transfer band in the near-UV (Rossman, 1984).

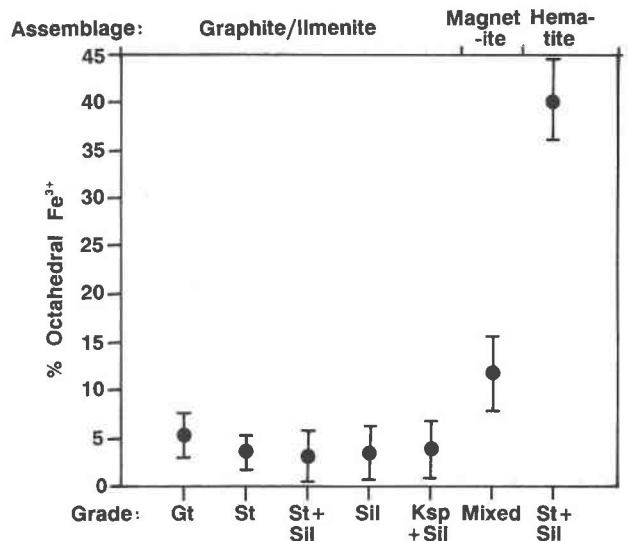


Fig. 4. Plot of octahedral Fe^{3+} vs. assemblage and oxide, showing a minimum $\text{Fe}_{\text{oct}}^{3+}$ content of about 4% of the total iron for graphite + ilmenite-bearing assemblages regardless of metamorphic grade. Error bars are calculated with standard deviations except for hematite grade (represented by a single sample), where error bar shown is estimated precision. Most variation in octahedral Fe^{3+} content above the 4% level occurs as a result of increasing oxidation state.

Absorption effects also arise from Fe^{3+} and Fe^{2+} in the octahedral sheet. Octahedral Fe^{2+} alone gives rise to absorption bands at 9000 and 11000 cm^{-1} , and the intensity of those bands increases nonlinearly as octahedral Fe^{3+} increases (Smith et al., 1980). An Fe^{3+} - Fe^{2+} charge-transfer band occurs around 14000 cm^{-1} . All three Fe bands (9000, 11000, and 14000 cm^{-1}) are commonly observed in spectra of biotite with high concentrations of Fe^{3+} , Fe^{2+} , and Ti^{4+} (Rossman, 1984).

The biotite samples in the present study fall into two groups: reddish orange samples containing only about 12% of the total iron as Fe^{3+} , and greenish brown biotite with higher total Fe^{3+} values. Any optical absorptions that might arise from tetrahedral Fe^{3+} in these samples are apparently small relative to the intensity of the Ti^{4+} - Fe^{2+} and Fe^{3+} - Fe^{2+} charge-transfer bands (Fig. 3). However, the red-orange color of the low Fe^{3+} biotites from the most reduced assemblages indicates the presence of Ti^{4+} - Fe^{2+} absorptions without any significant contribution from octahedral Fe^{3+} - Fe^{2+} . Further confirmation of this conclusion is the observation that the color of the biotites in the reduced rocks changes systematically as a function of Ti content. As Ti increases (with increasing metamorphic grade) the color changes from reddish orange to reddish brown to chestnut brown. Thus, the darkening reddish shades reflect the Ti increase (which results in increased Ti^{4+} - Fe^{2+} charge transfer) in a straightforward (though not necessarily linear) fashion.

The greenish brown color associated with octahedral Fe^{3+} - Fe^{2+} charge transfer is only observed in the biotite from the more oxidizing assemblages. This biotite contains just as much Ti as biotite from similar metamorphic grades with more reduced assemblages. Within a given metamorphic grade, bulk elemental compositions of biotites do not vary with oxidation state; therefore, the color difference can be directly related to the concentration and occupancy of Fe^{3+} . If Fe^{3+} is present in the octahedral sheet at levels above ~ 0.1 atoms/22 O atoms, there is significant Fe^{3+} - Fe^{2+} charge transfer, and the effects of the Ti^{4+} - Fe^{2+} interaction are no longer visible. Biotite conspicuously transmits in the 14000 cm^{-1} charge transfer region. Therefore, the color of the biotite with lower Fe^{3+} contents from reduced assemblages indicates a lack of significant octahedral Fe^{3+} in those samples. The assignment of Fe^{3+} to tetrahedral coordination based on Mössbauer data is therefore supported.

Variation over a range of metamorphic grade

Within the known errors of the Mössbauer technique, neither the Fe^{3+} contents nor the Fe^{2+} M2/M1 ratios of our micas display systematic variation that can be correlated with changing metamorphic conditions. Only one small group of samples appears to be distinctive. One subset of micas from the lower sillimanite grade in the Oquossoc quadrangle coexists with $>3\%$ modal pyrrhotite (samples O-K-9, O-K-8, and O-K-8'). As discussed in Guidotti et al. (1988), these samples have small Fe contents due to reactions in the rocks that draw Fe into

pyrrhotite. Although the total amount of Fe in these samples is low, the percentage of Fe^{3+} remains relatively constant. This is significant because it implies that the amount of tetrahedral Fe^{3+} per formula unit is not constant but varies with composition. These three samples show extremes of Fe^{2+} ordering that probably reflect the related increase in octahedral Mg. The fact that Fe^{2+} occupancies change significantly where Mg increases dramatically suggests that Mg may have a strong site preference, probably for M2 (M2/M1 ratios in O-K-8 and O-K-8' are 1.60 and 1.61, respectively). The slightly different bulk composition of O-K-9 yields a reverse M2/M1 ratio of 5.20. Regrettably, our three-sample data set does not provide sufficient information to explain why these extremes exist.

The amount of tetrahedral Fe^{3+} is nearly constant at an average of $8 \pm 2.5\%$ of the total Fe over the range of metamorphic grade studied. In the most reduced rocks, those from ilmenite + graphite assemblages, $\frac{2}{3}$ of the Fe^{3+} present accounts for the 8% present in the tetrahedral sites. Even in biotite samples from the more oxidizing environments in which $>15\text{--}20\%$ of the total iron is Fe^{3+} , only 8% goes into tetrahedral coordination, with the balance in octahedral coordination. This observation strongly suggests that tetrahedral Fe^{3+} is present because the structure requires it for stability; its existence is not related to the oxidation state of the assemblage. This idea is discussed in detail in the companion paper (Guidotti and Dyar, in preparation). Only the amount of octahedral Fe^{3+} varies systematically with the oxidation state in the rocks (Fig. 4).

CONCLUSIONS

Mössbauer spectra of 52 biotite samples from low garnet to potassium feldspar + sillimanite-grade metapelites in northwestern Maine show almost constant peak positions of Fe^{2+} in *cis*-M2 sites but greater variation in hyperfine parameters of Fe^{2+} in *trans*-M1. This observation suggests that the geometry of the M2 site is relatively constant, but that the average *trans*-M1 site is distorted to different degrees in different samples. This distribution may be caused by variation in the average number of octahedral vacancies or in the next-nearest-neighbor cations. Fe^{3+} peaks can sometimes be resolved as two distinct doublets corresponding to Fe^{3+} in the two types of octahedral sites. More frequently, the spectra are best fitted with a single combined octahedral Fe^{3+} doublet with hyperfine parameters representing averages of *cis*-M2 and *trans*-M1 and a total of about 4% of the total peak area. An average of 8% of the total iron occurs as tetrahedral Fe^{3+} in all of the samples studied. Its presence may be correlated with the number of octahedral vacancies.

Viewed in a petrologic context, these data assume greater significance. For the most part, $\text{Fe}^{3+}/\Sigma\text{Fe}$ and Fe^{2+} M2/M1 ratios do not vary over the broad range of metamorphic grade examined here, except in samples containing pyrrhotite. Octahedral Fe^{3+} content does increase in biotite from increasingly oxidized assemblages. The fact that the concentration of tetrahedral Fe^{3+} remains

constant over the wide range in metamorphic grade studied suggests that structural requirements within the biotite, rather than variation in oxidation state, are responsible for its presence.

ACKNOWLEDGMENTS

The author thanks Charles Guidotti for generously making his samples available for this study and Don Hickmott for making the suggestion that got this whole project started. Conversations with M. Reed, T. Grover, S. W. Bailey and S. Guggenheim and reviews by E. DeGrave, E. S. Grew, S. Guggenheim, R. K. Kirkpatrick and C. R. Rebbert are gratefully acknowledged. Thanks also to Roger Burns and George Rossman for use of their analytical facilities and for support of the author during the early stages of this work. I am indebted to Chryl Perry, Carolyn Rebbert, Kathleen Ward, and Dick Ziegler for assistance in data reduction and to Anne V. McGuire and Beth Holmberg of the Smithsonian Astrophysical Observatory, Cambridge, Massachusetts, for last-minute electron microprobe analyses needed to complete this paper. This work was supported through N.S.F. grants EAR-8709359 and EAR-8816935. Acknowledgment is also made to the donors of the Petroleum Research Fund, administered by the A.C.S., for additional support of this research through grant 19217-G2.

REFERENCES CITED

- Albee, A.L., and Ray, L. (1970) Correction factors for electron probe microanalysis of silicates, oxides, carbonates, phosphates, and sulfates. *Analytical Chemistry*, 42, 1408–1414.
- Bailey, S.W. (1984) Micas. *Mineralogical Society of America Reviews in Mineralogy*, 13, 584 p.
- Bancroft, G.M., and Brown, J.R. (1975) A Mössbauer study of coexisting hornblendes and biotites: Quantitative Fe³⁺/Fe²⁺ ratios. *American Mineralogist*, 60, 265–272.
- Bence, A.E., and Albee, A.L. (1968) Empirical correction factors for the electron microanalysis of silicates and oxides. *Journal of Geology*, 76, 382–403.
- DeGrave, E., Vandenbruwaene, J., and Van Bockstael, M. (1987) ⁵⁷Fe Mössbauer spectroscopic analysis of chlorite. *Physics and Chemistry of Minerals*, 15, 173–180.
- Dodge, F.C.W., Smith, V.C., and Mays, R.E. (1969) Biotites from granitic rocks of central Sierra Nevada batholith, California. *Journal of Petrology*, 10, 250–271.
- Dyar, M.D. (1984) Precision and interlaboratory reproducibility of measurements of the Mössbauer effect in minerals. *American Mineralogist*, 69, 1127–1144.
- (1987) A review of Mössbauer data on trioctahedral micas: Evidence for tetrahedral Fe³⁺ and cation ordering. *American Mineralogist*, 72, 102–112.
- Dyar, M.D., and Burns, R.G. (1986) Mössbauer spectra study of ferruginous one-layer trioctahedral micas. *American Mineralogist*, 71, 951–961.
- Dyar, M.D., Grover, T.W., Rice, J.M., and Guidotti, C.V. (1987) Presence of ferric iron and octahedral ferrous ordering in biotites from pelitic schists: Implications for garnet-biotite geothermometry. *Geological Society of America Abstract with Programs*, 19, 650.
- Dyar, M.D., Hickmott, D., Guidotti, C.V., and Cheney, J.T. (1986) M2/M1 ordering of iron in biotites from northwestern Maine. *International Mineralogical Association Abstracts*, 14, 94.
- Faye, G.H. (1968) The optical absorption spectra of certain transition metal ions in muscovite, lepidolite, and fuchsite. *Canadian Journal of Earth Sciences*, 5, 31–38.
- Ferrow, E. (1987) Mössbauer effect and X-ray diffraction studies of synthetic iron bearing trioctahedral micas. *Physics and Chemistry of Minerals*, 14, 276–280.
- Guggenheim, S. (1984) The brittle micas. In S.W. Bailey, Ed., *Micas. Mineralogical Society of America Reviews in Mineralogy*, 13, 61–104.
- Guidotti, C.V. (1984) Micas in metamorphic rocks. In S.W. Bailey, Ed., *Micas. Mineralogical Society of America Reviews in Mineralogy*, 13, 357–467.
- Guidotti, C.V., Cheney, J.T., and Guggenheim, S. (1977) Distribution of titanium between muscovite and biotite in metapelites from N.W. Maine. *American Mineralogist*, 62, 438–448.
- Guidotti, C.V., Cheney, J.T., and Henry, D.J. (1988) Compositional variation of biotite as a function of metamorphic reactions and mineral assemblage in the pelitic schists of western Maine. *American Journal of Science*, 288A, 270–292.
- Henry, D.J. (1981) Sulfide-silicate relations of the staurolite-grade pelitic schists, Rangeley quadrangle, Maine, 773 p. Ph.D. thesis. University of Wisconsin, Madison, Wisconsin.
- Huggins, F.E. (1976) Mössbauer studies of iron minerals under pressures of up to 200 kilobars. In R.A. Strens, Ed., *The physics and chemistry of minerals and rocks*, p. 613–640. Wiley, London.
- Levitz, P., Callas, G., Bonnin, D., and Legrand, A.P. (1980) Étude par spectroscopie Mössbauer du Fer(III) dans des verres silicatés multi-composants d'intérêt géologique. *Revue de Physique Appliquée*, 15, 1169–1173.
- Rossman, G.R. (1984) Spectroscopy of micas. In S.W. Bailey, Ed., *Micas. Mineralogical Society of America Reviews in Mineralogy*, 13, 61–104.
- Rossman, G.R., Grew, E.S., and Dollase, W.A. (1982) The colors of sillimanite. *American Mineralogist*, 67, 749–761.
- Ruby, S.L. (1973) Why misfit when you already have X²? In I.J. Gruverman and C.W. Seidel, Eds., *Mössbauer effect methodology*, 8, 263–276. Plenum Press, New York.
- Shannon, R.D. (1976) Revised effective ionic radii and systematic studies of interatomic distances in halides and chalcogenides. *Acta Crystallographica*, A32, 751–767.
- Smith, G., Howes, B., and Hasan, Z. (1980) Mössbauer and optical spectra of biotite: A case for Fe³⁺-Fe²⁺ interactions. *Physica Status Solidi*, A57, K187–K192.
- Stone, A.J., Parkin, K.M., and Dyar, M.D. (1984) STONE: A program for resolving Mössbauer spectra: DEC Users' Society Program Library, no. 11-720. Marlboro, Massachusetts.
- Wood, C. (1981) Chemical and textural zoning in metamorphic garnets, Rangeley Area, Maine, 586 p. Ph.D. thesis. University of Wisconsin, Madison, Wisconsin.

MANUSCRIPT RECEIVED JULY 5, 1989

MANUSCRIPT ACCEPTED FEBRUARY 28, 1990